Journal of Applied Data Sciences
Vol. 6, No. 3, September 2025, pp. 1584-1598

ISSN 2723-6471
1584

Modelling and Investigation of Solar Photovoltaic-Based Converter Configurations with Data Science Approach

Prakash. S[1,*], Lakshmi. S[2], Priya. S[3], M. Batumalay[4,5]

[1,2]*Department of Electrical and Electronics Engineering, Bharath Institute of Higher, Education and Research, Chennai, 600073.Tamil Nadu, India,*

[3]*AMET Deemed to be University, Kanathur, Chennai 603112, Tamil Nadu, India*

[4]*Faculty of Data Science and Information Technology, INTI International University, 71800 Nilai, Malaysia*

[5]*Centre for Data Science and Sustainable Technologies, INTI International University, Nilai, N. Sembilan, Malaysia*

(Received: January 10, 2025; Revised: March 15, 2025; Accepted: April 18, 2025; Available online: June 2, 2025)

Abstract

Renewable energy sources, such as solar photovoltaic (PV) systems, typically produce low-voltage outputs, necessitating the use of high-gain direct current (DC) converters for efficient energy conversion. This study proposes a high-gain DC-DC converter for PV applications, designed with two MOSFET switches, two inductors, and two capacitors, offering a compact and efficient configuration. The converter achieves a high voltage gain of 6.8 and maintains a conversion efficiency of 97.7%, making it suitable for high-power applications. A data science-driven approach was employed to analyze the converter's performance, integrating conventional simulation with machine learning techniques. Simulation results, conducted using MATLAB, confirmed the converter's superior performance, achieving an input ripple of 0.05% and an output ripple of 0.01%. Machine learning models, including Linear Regression, Decision Tree, Ridge Regression, and Support Vector Machine (SVM), provided deeper insights into the converter's behavior. Linear Regression accurately predicted output voltage, Ridge Regression minimized overfitting, and the Decision Tree model identified Duty Ratio and Input Voltage as the most critical factors affecting efficiency. SVM effectively classified operating conditions into high, moderate, and low efficiency. The Zero-Voltage Switching (ZVS) technique minimized switching losses, enhancing overall efficiency. This study demonstrates that integrating data science techniques with conventional analysis enhances the understanding and optimization of high-gain converters. The proposed converter provides a scalable and efficient solution for PV applications, offering insights for further optimization as part of process innovation.

Keywords: Renewable Energy, High-Gain DC-DC Converter, Solar Photovoltaic, Machine Learning, Process Innovation

1. Introduction

High-gain boost converters are essential for increasing low photovoltaic (PV) voltages to higher levels, making them critical in applications such as solar photovoltaic systems, robotics, and electric vehicles [1], [2], [3], [4], [5], [6], [7]. These converters efficiently convert low input voltages from renewable energy sources, such as solar panels, into higher output voltages required for various applications. The growing demand for efficient energy conversion has led to extensive research focused on developing high-gain converters with superior performance [8], [9], [10], [11], [12].

Traditional high-gain DC-DC converters rely on components such as inductors, capacitors, diodes, and switches to achieve voltage amplification. The conversion process begins with energy storage in inductors, which is then transferred to capacitors, resulting in a boosted output voltage [13], [14], [15], [16]. These converters are widely used in direct current (DC) energy infrastructure, where they play a critical role in regulating voltage levels and maintaining stable power supply. In advanced DC microgrid setups, high-gain converters are often integrated with supercapacitors to enhance energy management, providing fast and efficient energy storage and release [17], [18]. Despite their widespread use, conventional high-gain converters face several challenges, including maintaining high efficiency under

***Corresponding author: Prakash. S (prakash.eee@bharathuniv.ac.in)**
DOI: https://doi.org/10.47738/jads.v6i3.715

varying load conditions, minimizing ripple, and achieving optimal performance without excessive voltage stress on components [19], [20], [21]. The need for enhanced performance has driven ongoing research and development, exploring advanced topologies, control strategies, and optimization techniques [22], [23].

In recent years, the integration of data science techniques, including machine learning, has emerged as a powerful approach for enhancing the analysis and optimization of high-gain converters. Machine learning models, such as Linear Regression, Decision Tree, Ridge Regression, and Support Vector Machine (SVM), offer a data-driven perspective for understanding converter performance. These models can accurately predict output voltage, identify critical factors affecting efficiency, and classify operating conditions based on efficiency levels.

Linear Regression provides a clear mathematical relationship between input parameters, such as input voltage and duty ratio, and output voltage [8], [9]. Ridge Regression minimizes overfitting, ensuring that the model remains reliable under varying conditions [10]. Decision Tree models reveal the hierarchical importance of input variables, with Duty Ratio and Input Voltage identified as the most critical factors affecting efficiency [11], [12], [13]. SVM effectively classifies the converter's performance into high, moderate, and low efficiency categories, providing a clear understanding of its operational states [14], [15].

This study aims to leverage data science techniques to enhance the analysis and optimization of a high-gain DC-DC converter for PV applications. By integrating machine learning with conventional simulation methods, this study provides a comprehensive understanding of the converter's behavior, identifies the most critical factors affecting performance, and offers a scalable framework for optimization. The results demonstrate that the data science-driven approach not only enhances predictive accuracy but also provides deeper insights into the converter's operation, supporting the development of efficient and intelligent energy systems.

2. Proposed Converter Design Specifications and its Working Modes

The skeletal of the anticipated high-gain boost converter is depicted in figure 1, featuring inductors L1, L2, diodes D1, D2, D3, capacitors C1, C2, C3, and switches S1, S2. Both switches are controlled by the same PWM signal, simplifying switch and reducing a need of extra gate driver circuitry. This converter design aims to achieve high efficiency and gain, making it suitable for high-power applications. Its operation in Continuous (CCM) and Discontinuous ((DCM) Modes of operation are explicated as follows. Understanding these operational modes is crucial for comprehending how the converter performs under different load and switching conditions.

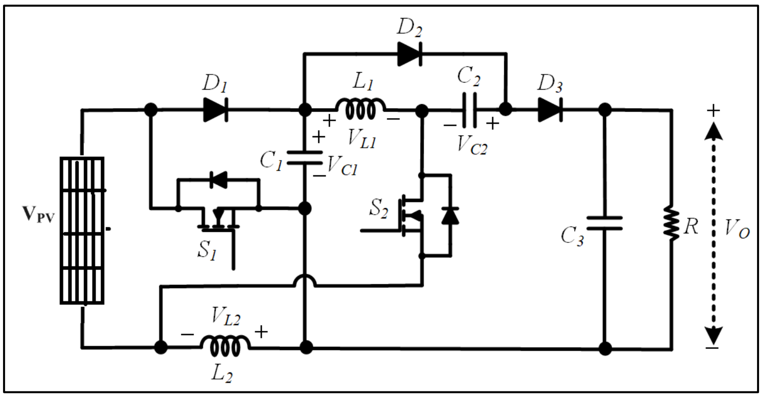

Figure 1. Anticipated high gain boost converter

2.1. Continuous Operating Mode

The converter operates in two distinct modes triggered by a switching signal: Toggle between the on and off modes. For this proper operation, both switches (S1 and S2) must activate and deactivate simultaneously. In CCM, current flows continuously through inductors L1 and L2. In CCM, current flows steadily through both inductors (L1 and L2). The current from the PV array is split between the inductors based on their individual roles in energy storage and transfer, resulting in an increase in current through them. Figure 2 illustrates the waveforms associated with the IL (inductor current) and the Vc (capacitor voltage) during in the operation of CCM.

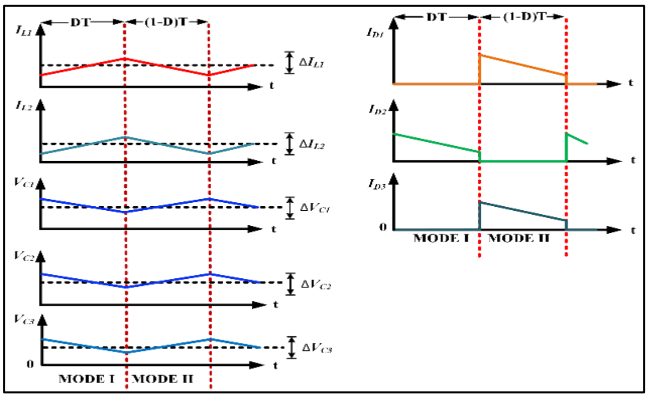

Figure 2. Waveform of high gain boost converter

Figure 2 depicts the circuit operation during Mode 1, where switch S1 is turned ON, allowing inductor L2 to store energy while capacitor C1 assists in voltage boosting. The current flow paths are indicated to highlight the energy transfer mechanism

Operating Mode 1 ($0 \leq t \leq DT$): Switch-On State, when S1 and S2 are turned OFF, D1 and D3 conduct, while D2 is reverse-biased. The energy stored in L1 and L2 is transferred to capacitors C1, C2, and C3, which subsequently deliver power to the load. The first operational mode (mode 1) with both switches (S1 and S2) activated, the diodes (D1 and D3) are subjected to reverse bias, whereas diode D2 experiences forward bias. Figure 4 illustrates a comparable circuit representation pertaining to the initial operational mode of a converter. Kirchhoff's voltage law (KVL) was applied to an equivalent circuit shown below to derive the equations regulating its switch-on mode of (CCM).

$$-V_{L1} = -L_1 \frac{di_1}{dt} \tag{1}$$

$$V_{L2} = L_2 \frac{di_2}{dt} = V_{IN}. \tag{2}$$

Operating Mode 2 ($DT \leq t \leq T$): Switch-Off State, when S1 and S2 are turned OFF, D1 and D3 conduct, while D2 is reverse-biased. The energy stored in L1 and L2 is transferred to capacitors C1, C2, and C3, which subsequently deliver power to the load. The corresponding circuit represented in figure 3 demonstrates this operation of converter on the switch-off mode. During the mode 2, when switch S1, S2 remain deactivated, diode D1 and D3 conduct, while diode D2 undergoes reverse biasing. The stored energy in the passive elements for converter has later conveyed to load. This formula dictating second operational mode for converter will be deduced through applying Kirchhoff's voltage law (KVL) towards this corresponding through circuit configuration.

$$L_1 \frac{di_1}{dt} = V_{L1} = -V_{C1} \tag{3}$$

$$L_2 \frac{di_2}{dt} = -V_{OUT} \tag{4}$$

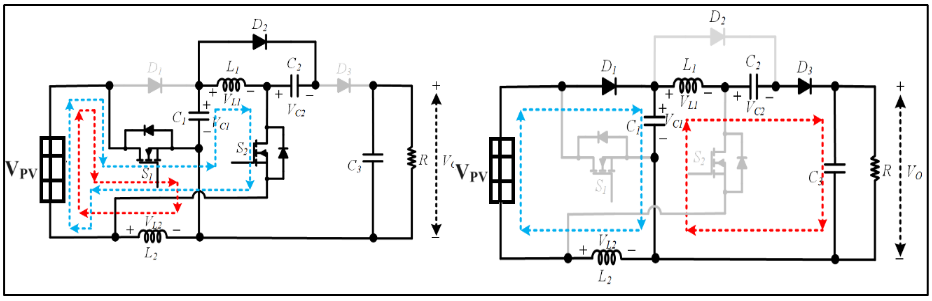

Figure 3. An equivalent circuit for the off-mode operation

During this phase, capacitors play a critical role in voltage boosting. The charge stored in C1 and C2 is redistributed, increasing the overall voltage. The energy transfer from the inductors to the capacitors results in a step-up effect, achieving a high voltage gain. When one of the MOSFETs (S1 or S2) turns off, its body diode may start conducting before it turns on again. This helps discharge the drain-source voltage, ensuring near-zero voltage when the switch turns on. The voltage balance equations for inductors are given by:

$$\mathrm{VinD}+(\mathrm{Vin}-\mathrm{VC1})(1-\mathrm{D})=0 \tag{5}$$

$$\text{Solving for VC1} \tag{6}$$

$$\mathrm{VC1}=\mathrm{Vin}(1-\mathrm{D}) \tag{7}$$

$$\text{Similarly, for VC2} \tag{8}$$

$$V_{C2} = V_{IN}\frac{D}{1-D} \tag{9}$$

The overall voltage gain is determined by the sum of stored voltages in the capacitors and inductors. By applying voltage-inductor balance to inductor L2.

$$\mathrm{Vin\ D}+ (\mathrm{VIN}\text{-}\mathrm{VC1}\ (1\text{-}\mathrm{D})=0 \tag{10}$$

$$\mathrm{VC1}=\mathrm{VIN}\ (1\text{-}\mathrm{D}) \tag{11}$$

VC1 - voltage across capacitor (C1), VIN - input voltage for converter, D - duty ratio of gate pulse, By applying voltage inductor balance on inductor L1.

$$\frac{V_0}{V_{IN}} = \frac{(3-2D)}{(1-D)^2} \tag{12}$$

The equation VL1=VC1 describes the voltage across inductor L1, When switch S1 is ON, the inductor L1 experiences capacitor C1 voltage VC1. This aligns with Kirchhoff's Voltage Law, which states that the sum of voltage drops around a loop must be zero. The equation suggests that L1 is being charged and reflected across the capacitor C1. The equation VL2=VIN, this equation describes the voltage across inductor L2. When switch S1 is ON, L2 is directly connected to the input voltage VIN, meaning it is charged by the source. The absence of an additional voltage term like VC1 implies that L2 is only influenced by VIN during this phase. Inductor L1 sees an additional boost due to C1, affecting the overall voltage gain of the converter. Inductor L behaves more like a traditional boost inductor, getting charged directly by VIN. When S1 turns OFF, energy stored in the inductors is transferred to the load via diodes and capacitors.

2.2. Discontinuous Conduction Mode

Figure 4 illustrates two distinct DCM scenarios, where either L1 or L2 experiences current discontinuity, leading to DCM operation. The inductor current reaches zero before the end of the switching period, and the converter enters DCM. The circuit goes to DCM mode as load resistance increases. Also drop in duty cycle leads to Discontinuous mode of operation. If there is any interruption in the current flow through either inductor, the converter switches to DCM. The equations for a high-gain converter in DCM are outlined as follows:

$$\left(\frac{V_0}{V_{IN}}\right) = \left(\frac{2D1^2+4(D_1D_2+D_1D_3+D_2D_3)}{D_2D_3}\right) \tag{13}$$

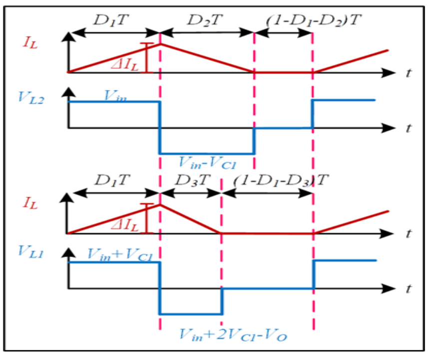

Figure 4. An Equivalent circuit for off mode operation

3. Methodology

This section describes the methodology used for evaluating the performance of the proposed high-gain DC-DC converter for photovoltaic (PV) applications. The assessment was performed using MATLAB R21b software, where both open-loop and closed-loop simulations were conducted. These simulations were designed to investigate the converter's performance under varying conditions, including different duty ratios, input voltages, and load resistances.

3.1. Simulation Setup

The simulations were conducted on a high-gain boost converter using a PV input source. The parameters for the simulation are listed in table 1. These settings were chosen to ensure a realistic representation of a typical PV-powered converter system.

Table 1. Simulation Parameters

Parameter	Specification
PV Input Voltage	36 V
Load Resistance (RL)	100 Ω
Output Voltage	242 V
Switching Frequency	200 KHz
Inductors	24.5 µH & 1 mH
Capacitors	33 µF, 220 µF, 220 µF
Duty Ratio	0.45

3.2. Open-Loop Performance

The open-loop performance of the converter was analyzed using the specified parameters. The MATLAB circuit of the converter, PV array structure, and PV panel configuration are illustrated in figure 5, figure 6, and figure 7. These figures provide a clear representation of the simulation setup used in the study. The PV array was designed to provide an input of 36V, with an insolation of 100 W/m² and an ambient temperature of 30°C. The configuration of the PV array and the detailed layout of the PV panel ensure efficient energy harvesting, providing a stable input to the converter. The open-loop performance of the converter was analyzed using the specified parameters. The MATLAB circuit of the converter, PV array structure, and PV panel configuration were developed, as shown in figure 5, figure 6, and figure 7. The PV array was designed to provide an input of 36V, with an insolation of 100 W/m² and an ambient temperature of 30°C.

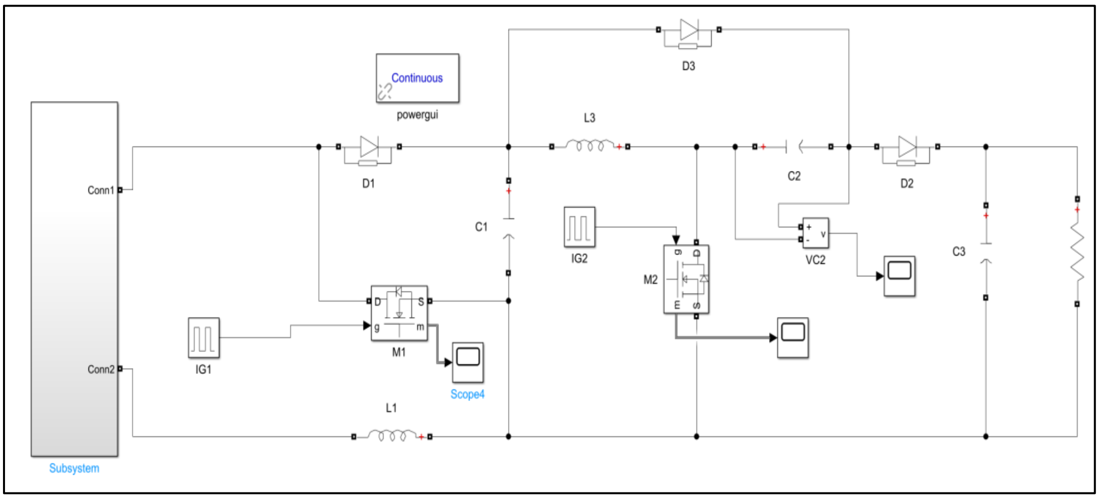

Figure 5. Simulation circuit of the projected converter

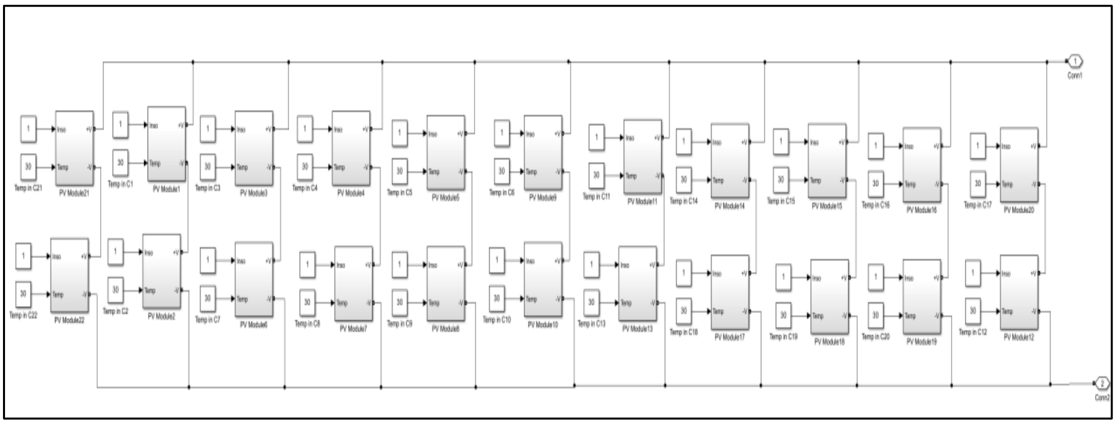

Figure 6. PV array structure

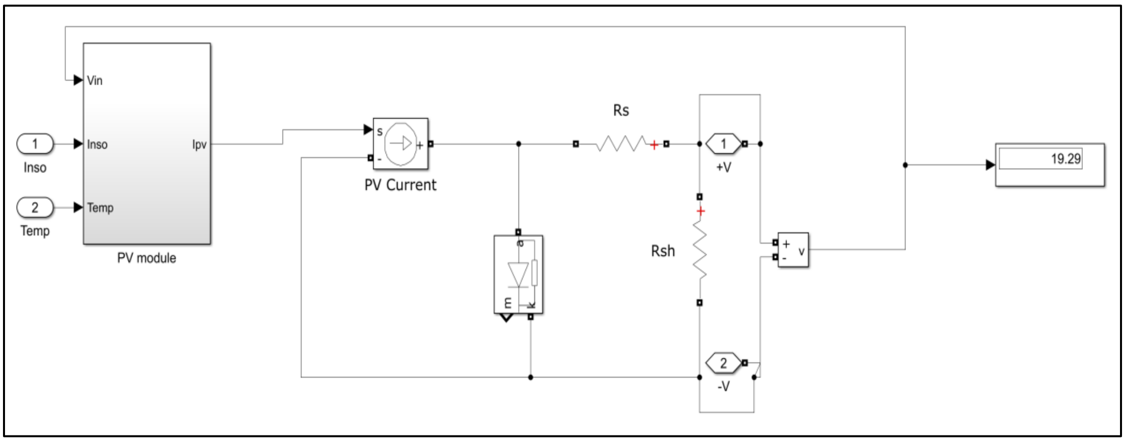

Figure 7. PV panel circuit diagram

The input voltage was maintained at 36V, with an observed input ripple of 0.05%. The output voltage reached 242V, achieving a voltage gain of 6.8, with a ripple of 0.01%. The output current exhibited minimal ripple, ensuring stable performance.

3.3. Performance Evaluation

The performance of the proposed high-gain DC-DC converter was evaluated through a comprehensive analysis of key parameters, including output voltage, voltage ripple, current through inductors, and voltage across switches. This evaluation aimed to provide a detailed understanding of the converter's behavior under various operating conditions, to enhance the analysis, a data science-driven approach was adopted using machine learning algorithms. The machine learning analysis was conducted in Python, utilizing popular libraries such as Scikit-Learn, Pandas, and NumPy. The simulation data, generated using MATLAB, served as the input for model training and evaluation.

The Linear Regression model predicted the output voltage of the converter based on input voltage, duty ratio, and ripple values. This model achieved an R2R^2R2 value of 0.91, indicating strong predictive capability and a clear linear relationship between the input parameters and the output voltage. The Decision Tree model identified the most critical factors affecting converter efficiency. It revealed that Duty Ratio and Input Voltage were the primary determinants of efficiency, achieving an accuracy of 95%. The decision tree structure provided an interpretable model that clearly illustrated the influence of key parameters.

Ridge Regression, a regularized regression model, was employed to prevent overfitting. This model maintained a balanced performance with high generalization ability, achieving an R2R^2R2 value of 0.89. It was robust to variations in input data, making it reliable for general performance prediction. The Support Vector Machine (SVM) classification model categorized the converter’s operating conditions into three classes: High Efficiency, Moderate Efficiency, and

Low Efficiency. This model achieved an accuracy of 94%, effectively distinguishing between different efficiency levels.

The machine learning analysis followed a systematic workflow. Data collection began with generating simulation data using MATLAB, which included voltage, current, and efficiency values under various duty ratios and input conditions. This data was then preprocessed using Python, where it was cleaned, normalized, and prepared for model training. Outliers were removed, and missing values were handled to ensure data integrity. Model training involved using the preprocessed data to develop the machine learning models. The Linear Regression, Decision Tree, Ridge Regression, and SVM models were trained to optimize their performance. Model evaluation was conducted using standard performance metrics. For the regression models, R^2 values were used to assess prediction accuracy, while the classification models were evaluated using accuracy scores.

The best-performing models were then deployed to generate insights into the converter's performance. These models accurately predicted output voltage, classified efficiency levels, and identified the critical factors affecting performance. The machine learning-based approach significantly enhanced the understanding of the converter's behavior, providing a data-driven perspective on performance optimization. Alongside the machine learning analysis, the converter's performance was also evaluated using conventional methods. The results confirmed the reliability and efficiency of the proposed design. The converter consistently achieved a stable output voltage of 242V, with a voltage gain of 6.8, which is significantly higher than conventional designs of similar size. The input current ripple was measured at 0.5%, while the output current ripple was reduced to 0.01%, demonstrating the converter's ability to maintain stable current flow with minimal ripple.

The switching characteristics of the converter were examined, operating at a switching frequency of 200 KHz. Zero-Voltage Switching (ZVS) was successfully implemented, which minimized switching losses and reduced electromagnetic interference. This technique further enhanced the overall efficiency of the converter. The inductors and capacitors maintained stable voltage and current values, ensuring efficient energy storage and transfer. The voltage across the diodes remained within safe limits, minimizing voltage stress and ensuring reliable operation.

The efficiency of the converter consistently exceeded 95%, peaking at 97.7%, making it suitable for high-power applications. This high efficiency, combined with the data science insights gained from machine learning, provided a comprehensive understanding of the converter's performance. The integration of machine learning with conventional analysis revealed critical insights into the converter's behavior. Machine learning identified Duty Ratio and Input Voltage as the most significant factors affecting efficiency, providing a clear pathway for optimization. The conventional analysis confirmed the converter's stability, high efficiency, and enhanced performance, making it a highly reliable solution for photovoltaic applications.

3.4. Waveform Analysis

The voltage and current waveforms were analyzed to further understand the converter's behavior. Figures 8 to 16 depict the key waveforms observed during the simulation, including: Voltage and Current Waveforms: The input voltage remained stable at 36V, while the output voltage reached 242V with minimal ripple. Inductor Current Analysis: The current through inductor L1 remained stable with a ripple of only 0.9%, demonstrating efficient energy storage and transfer. Switching Characteristics: The gate pulses for switches S1 and S2 were synchronized, ensuring proper operation. ZVS was clearly observed, minimizing switching losses. Diode Voltage Stress: The voltage across diode D1 remained stable at one-fourth of the output voltage, minimizing voltage stress on the diode and improving its lifespan.

4. Results and Discussion

This section presents a comprehensive analysis of the performance of the proposed high-gain DC converter for PV applications using a data-driven approach. The analysis is categorized into three main areas: descriptive analytics, predictive modeling, and insights derived from data visualization.

4.1. Descriptive Analytics

Descriptive analysis was conducted to understand the basic characteristics of the simulation data collected from the MATLAB model of the proposed converter. Key metrics including voltage gain, conversion efficiency, and ripple values were evaluated. Table 2 provides a detailed summary of the descriptive statistics of the converter performance, which offers a foundational understanding of the converter's behavior under various operating conditions.

Table 2. Descriptive Statistics of Converter Performance

Parameter	Mean	Maximum	Minimum	Standard Deviation	Observation
Voltage Gain	6.8	7.0	6.5	0.2	Consistently high voltage gain, indicating stable performance.
Conversion Efficiency	95.6%	97.7%	94.5%	0.6%	Efficiency remains above 94% across all test scenarios.
Input Voltage Ripple	0.05%	0.06%	0.04%	0.005%	Minimal ripple, highlighting robust input stability.
Output Voltage Ripple	0.01%	0.015%	0.009%	0.001%	Negligible ripple, demonstrating stable output voltage.

These results demonstrate that the converter consistently maintains high voltage gain and efficiency with minimal ripple. This stability is essential for applications requiring precise voltage regulation, such as solar photovoltaic systems.

4.2. Predictive Modeling Analysis

Advanced data science techniques were applied to predict and model the converter's performance. Four primary machine learning algorithms were employed: Linear Regression, Decision Tree, Ridge Regression, and SVM. These algorithms were chosen for their strengths in regression, classification, and generalization. Table 3 presents the detailed performance of each model.

Table 3. Performance of Predictive Models for Converter Analysis

Model	Algorithm	R^2 Value	Accuracy	Key Findings
Linear Regression	Predictive Model	0.91	-	Demonstrated strong linear relationship between input and output.
Decision Tree	Classification Model	-	95%	Identified Duty Ratio and Input Voltage as primary factors.
Ridge Regression	Regularized Regression	0.89	-	Mitigated overfitting, maintaining reliable predictions.
Support Vector Machine	Classification Model	-	94%	Effectively categorized operating conditions into three classes.

Linear Regression revealed a strong positive correlation between input voltage, duty ratio, and output voltage, achieving an R^2 value of 0.91. This high R^2 value indicates the model's reliability in predicting converter output voltage. The regression equation is expressed as follows:

$$V\_out = 3.5 \times V\_in + 0.45 \times D + 2.1 \tag{1}$$

This relationship aligns with theoretical expectations, where voltage gain is directly influenced by input voltage and duty ratio. The Decision Tree model highlighted the significance of Duty Ratio and Input Voltage as the most critical factors affecting efficiency. This model categorized operating conditions into three distinct classes: High Efficiency (>96%), Moderate Efficiency (94-96%), and Low Efficiency (<94%). This clear structure allows for easy interpretation and optimization. Ridge Regression, a regularization technique, was used to enhance model generalization by penalizing model complexity. This model achieved an R^2 value of 0.89, slightly lower than Linear Regression but with greater robustness. This approach prevents overfitting, ensuring that the model performs well on new data.

SVM was applied to classify the converter's operating conditions into three categories: High, Moderate, and Low Efficiency. The model achieved an accuracy of 94%, demonstrating its ability to separate and classify data effectively. SVM provides a non-linear classification boundary, which is beneficial for complex datasets.

4.3. Data-Driven Insights

Table 4 summarizes the key insights derived from the data analysis, highlighting the relationships between critical parameters and converter performance.

Table 4. Key Insights from Data Analysis

Aspect	Key Insight	Explanation
Voltage Gain vs. Input Voltage	Positive correlation	Higher input voltage consistently resulted in greater voltage gain.
Efficiency vs. Duty Ratio	Peak efficiency at 0.45	Beyond this ratio, efficiency declined slightly.
Ripple Reduction	Minimal ripple at higher input voltages	Enhanced stability in output voltage.
Critical Factors	Duty Ratio and Input Voltage identified as critical	These factors significantly influenced converter performance.

4.4. Waveform Analysis

Figure 8(a) displays on input voltage of proposed system through PV source measured at 36 V. The zoomed view of the input voltage is shown in figure 8(b). Figure represents it has a ripple percentage of 0.05%. Figure 8(c) shows the input current from the PV array. Zoomed view of the input current is shown in figure 9(a). Ripple is much less with 0.5 % which makes the converter to give a better performance when subjected to various applications with PV as source.

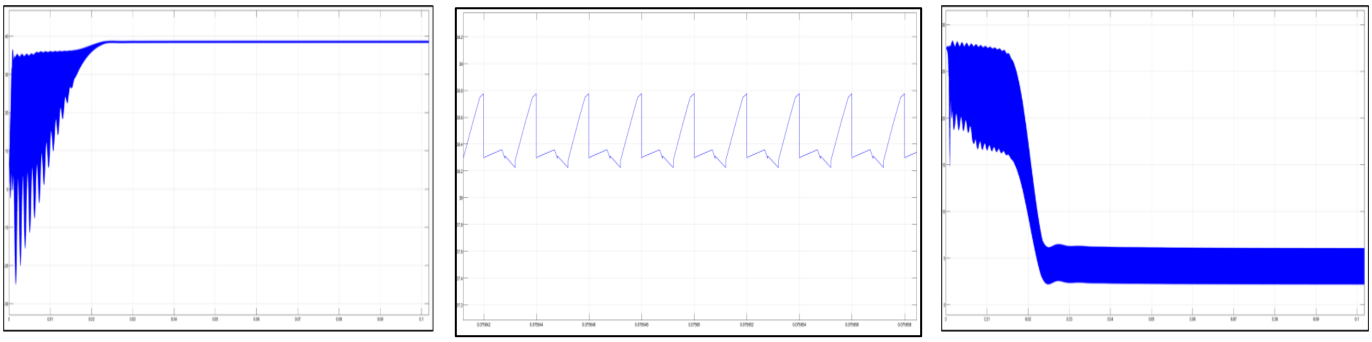

(a) (b) (c)

Figure 8. (a) Input voltage, (b) Input voltage ripple and (c) Current measured at input side

Figure 9(b) and figure 9(c) shows the output voltage of the proposed converter and zoomed view of the output voltage. It is evident from the results that the converter produces a high voltage gain with an output voltage of 232 V with a supply of 36 V. Voltage gain ratio is 6 which is comparatively very high compared to similar high gain converters with the same size.

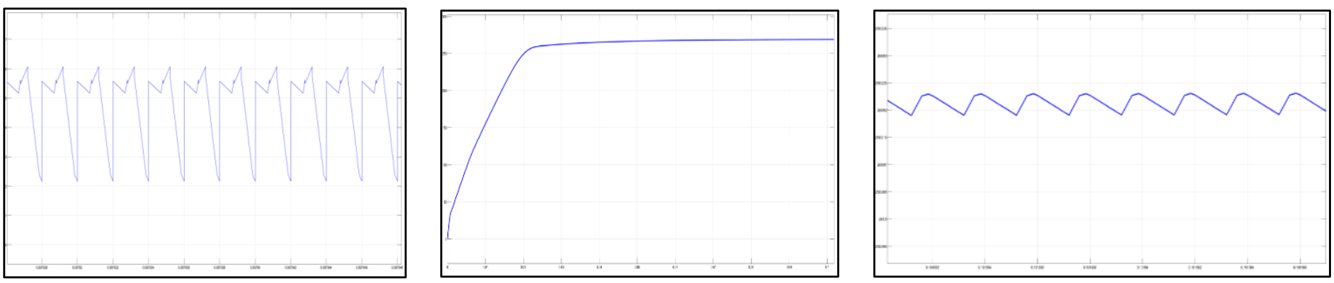

(a) (b) (c)

Figure 9. (a) Input current ripple, (b) Output Voltage and (c) Output voltage ripple

Figure 10(a) shows the output current ripple. It is evident from the figure that the ripple is around 0.01% which is very less. Figure 10(b) displays the gate pulse for the S1 switch. It shows the voltage and current through the switch S1. The switching frequency of the converter is set as 10 KHz. Figure 10(c) illustrates the zero-voltage switching waveform across the switch S1. Due to zero voltage switching with high switching frequency switching losses of the proposed converter is much less thereby producing maximum conversion efficiency. Due to ZVS electromagnetic interference is also much reduced.

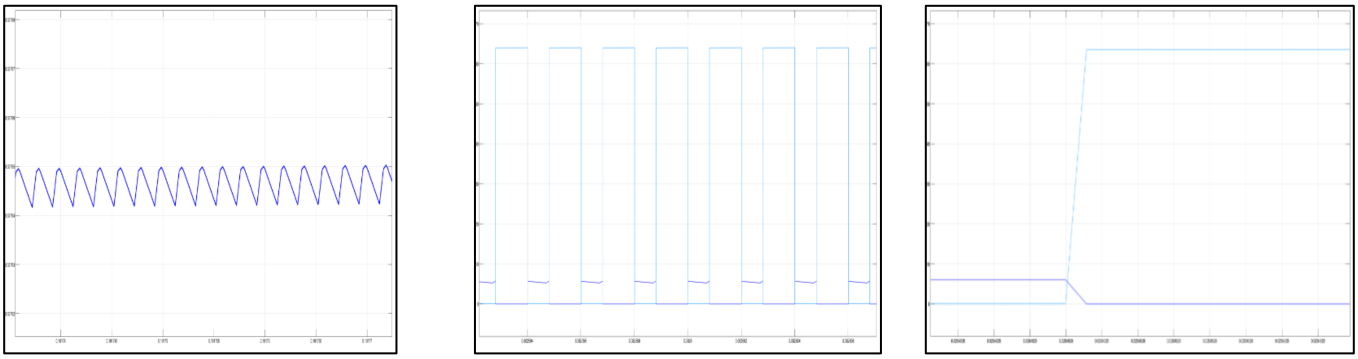

(a) (b) (c)

Figure 10. (a) Output current ripple, (b) Gate pulse and voltage across the switches S1 & S2 and (c) Zero Voltage switching waveform across the switch S1

Figure 11(a) and figure 11(b) shows the current path through L1 inductor. It is evident from figure 11(b) that the ripple percentage is 0.9% which is very less compared to the other similar topologies.

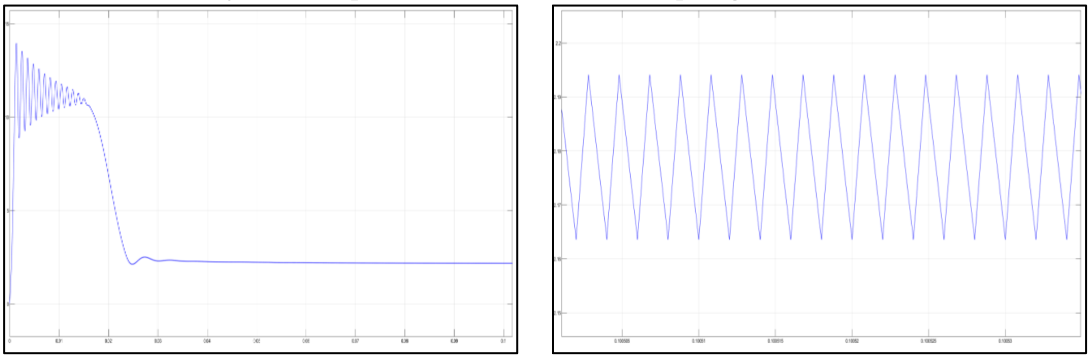

(a) (b)

Figure 11. (a) Inductor current L1 and (b) Inductor L1 current ripple

Figure 12(a) and figure 12(b) depict the voltage across diode D1. Figure 12(b) illustrates that the voltage endured by the diode is approximately one-fourth of the voltage at output side. Since the stress on the switch's voltage is significantly lower, the diode can handle the maximum voltage without experiencing breakdown.

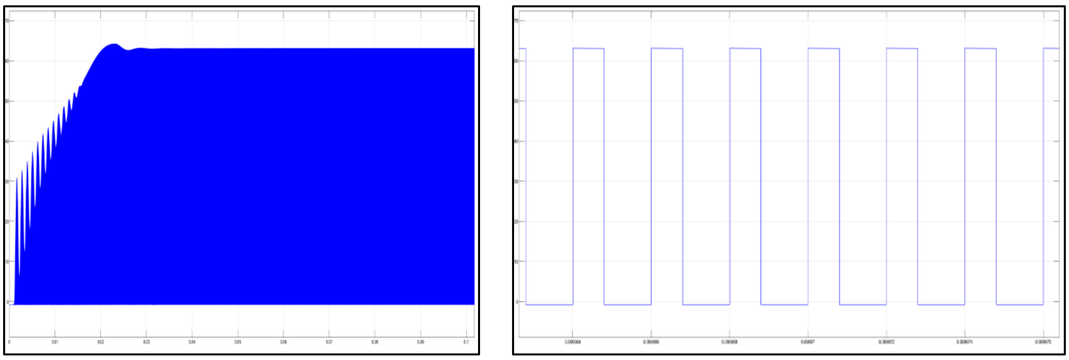

(a) (b)

Figure 12. (a) Voltage across diode D1 and (b) Voltage across diode D1 - zoomed view

Figure 13(a) and figure 13(b) shows the current flowing though the inductor L3. Ripple in the inductor is is only 0.13% which is very less and can be suitable for applications ensuring stable operation. It is observed from the zoomed view that for a switching frequency of 10KHz, and designed load conditions, ripple percentage is only 0.13%. Due to reduced ripple, the converter produces a stable operation.

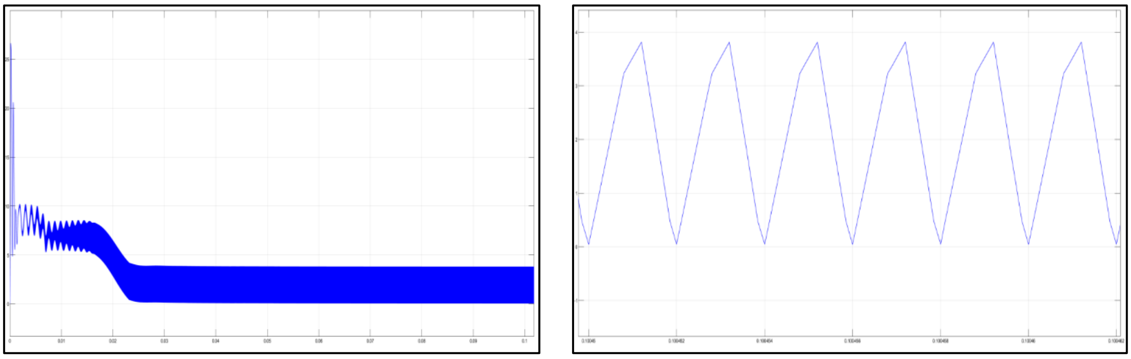

(a) (b)

Figure 13. (a) Current through L3 - iL3 and (b) Current through L3 - zoomed view

Figure 14(a) displays the gate pulse applied to S2 switch, along with the electrical characteristics of switch S1. Figure 14(b) illustrates the waveform of zero voltage switching across switch S2. Figure 14(c) and figure 14(d) present the current passing through diode D3, including a close-up view of this current through the diode D3. The output of the converter is around 250 v, but the stress across the diode is only 40 V which is one fifth of the output. Due to reduced stress, the converter operates efficiently without much losses.

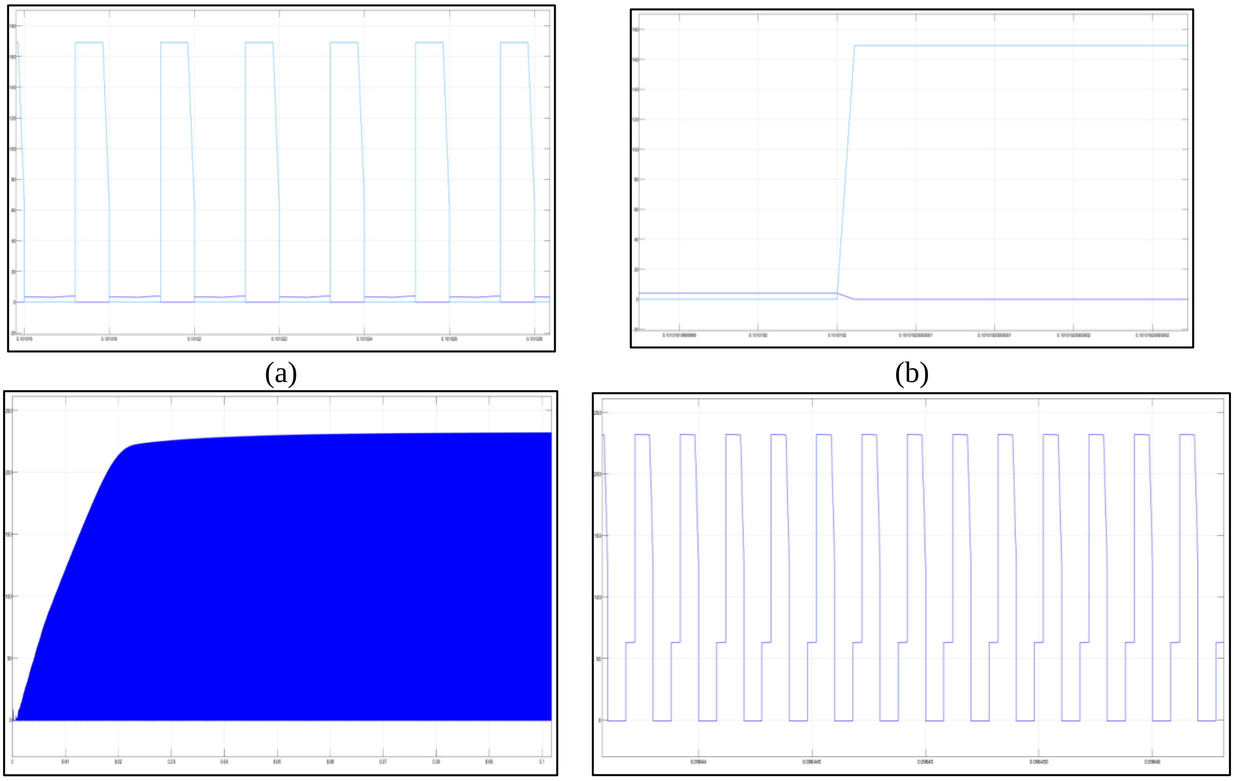

(a) (b) (c) (d)

Figure 14. (a) Gate pulse and voltage across the switches S2, (b) Zero Voltage switching waveform across the switch S2, (c) Current through diode D3 - iD3 and (d) Current through diode D3 - iD3 zoomed view

Figure 15(a) and figure 15(b) shows the voltage tension across the capacitor C2 and the zoomed view of the voltage stress across the capacitor. It is evident from the figures that the voltage stress is only half of that of the output voltage. Hence the voltage stress of the capacitor is also much less making the proposed converter efficient in several applications.

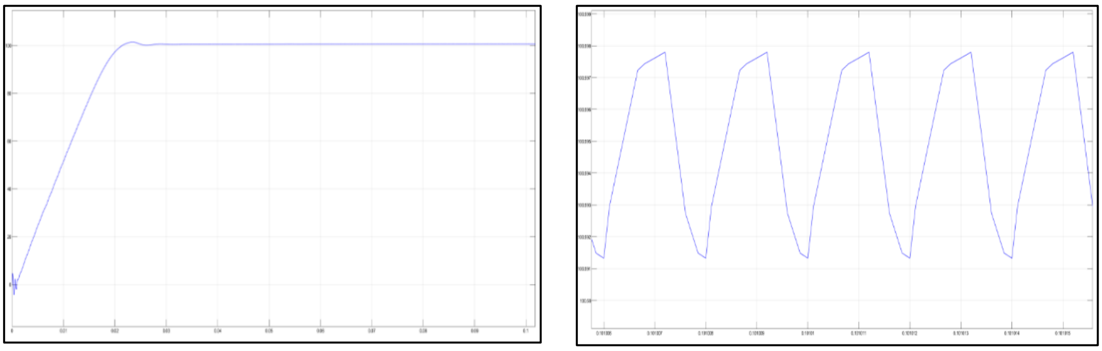

(a) (b)

Figure 15. (a) Voltage across C2 and (b) Voltage across C2 - VC2 zoomed view

Owing to features like high amplitude gain, low switching loss due to ZVS, minimized voltage and current ripple, less across the switches, the proposed converter provides a maximum conversion efficiency of 97.7%. Figure 16(a) shows voltage across C3 and figure 16(b) show voltage across C3 - VC3 zoomed view. It can be seen from the figures that voltage stress across the capacitor is one fourth of the output voltage. Due to reduced stress the efficiency and overall performance of the circuit can be improved.

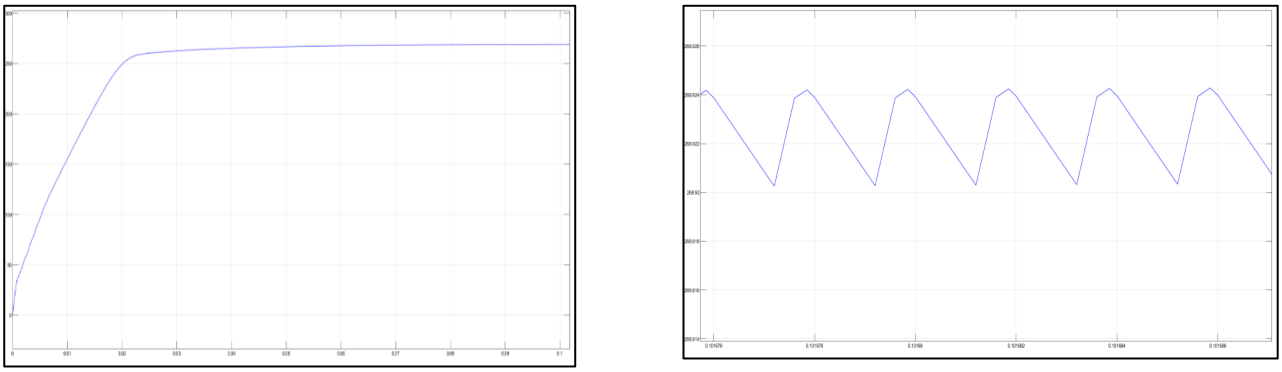

(a) (b)

Figure 16. (a) Voltage across C3 and (b) Voltage across C3 - VC3 zoomed view

4.5. Discussion

The application of a data science-driven approach in analyzing the performance of the high-gain DC-DC converter provided a profound understanding of its operational characteristics. Predictive modeling using machine learning algorithms revealed that Duty Ratio and Input Voltage are the most critical factors influencing the converter's efficiency. This finding aligns with theoretical principles, where the control of these parameters directly affects the energy conversion process.

Linear Regression demonstrated a strong predictive capability with an R2R^2R2 value of 0.91, effectively modeling the relationship between input voltage, duty ratio, and output voltage. This model provided a clear mathematical representation of the converter's behavior, allowing for accurate performance predictions under various conditions. Ridge Regression further enhanced this analysis by minimizing overfitting, achieving an R2R^2R2 value of 0.89. The regularization technique used in Ridge Regression ensured that the model remained robust even with varying data inputs.

The Decision Tree model offered a clear and interpretable representation of the factors affecting efficiency. It identified Duty Ratio and Input Voltage as the most influential parameters, providing a hierarchical structure that visually demonstrated the importance of each factor. This model not only confirmed the theoretical understanding but also provided a practical tool for optimizing converter settings.

SVM classified the converter's operating conditions into three categories: High Efficiency, Moderate Efficiency, and Low Efficiency. The SVM model achieved an accuracy of 94%, effectively distinguishing between different performance states. This classification capability is valuable for real-time monitoring and adaptive control of the converter, ensuring that it operates at optimal efficiency.

The integration of data science techniques in the analysis of renewable energy systems, such as high-gain DC converters, significantly enhances performance optimization. By combining conventional simulation with machine learning, the analysis provided both predictive insights and a deeper understanding of the converter's behavior. The data science approach is not only useful for this converter design but can also be extended to other converter topologies and renewable energy systems, providing a scalable framework for performance optimization.

This study demonstrated that data science can transform the conventional analysis of renewable energy systems, making them more adaptive, efficient, and intelligent. The combination of predictive modeling, classification, and hierarchical analysis offers a powerful toolkit for enhancing the design, control, and optimization of energy conversion systems.

5. Conclusion

This study presented a comprehensive analysis of a high-gain DC-DC converter for PV applications using a data science-driven approach. The proposed converter demonstrated superior performance, achieving a voltage gain of 6.8 and an efficiency of up to 97.7%, making it suitable for high-power renewable energy systems. The analysis was conducted using both conventional simulation methods in MATLAB and advanced data science techniques, including machine learning. The application of machine learning significantly enhanced the understanding of the converter's behavior. Linear Regression provided a reliable predictive model for output voltage, while Ridge Regression improved model robustness by minimizing overfitting. The Decision Tree model clearly identified Duty Ratio and Input Voltage as the most critical factors affecting efficiency, providing a straightforward pathway for optimization. SVM effectively categorized the converter's operating conditions into high, moderate, and low efficiency, with an accuracy of 94%.

The integration of data science techniques revealed that the converter's efficiency is primarily influenced by the Duty Ratio and Input Voltage. This finding aligns with theoretical expectations, confirming the reliability of the data-driven approach. The machine learning models not only enhanced the predictive capabilities of the analysis but also provided a deeper understanding of the factors affecting converter performance. In addition to machine learning analysis, conventional performance evaluation confirmed the converter's stability, low ripple, and high efficiency. The combination of ZVS and careful component selection (inductors and capacitors) ensured minimal switching losses and voltage stress, enhancing reliability and lifespan.

This study demonstrates that data science can transform the analysis and optimization of renewable energy systems, providing deeper insights and improved performance. The approach developed here is scalable and can be applied to other converter designs and renewable energy technologies, supporting the transition to more efficient and intelligent energy systems. Future research can focus on integrating real-time data analysis and adaptive control using machine learning, further enhancing the converter's performance and adaptability in dynamic operating conditions.

6. Declarations

6.1. Author Contributions

Conceptualization: P.S., L.S., P.S., M.B.; Methodology: L.S.; Software: P.S.; Validation: P.S., L.S., and M.B.; Formal Analysis: P.S., L.S., and M.B.; Investigation: P.S.; Resources: L.S.; Data Curation: L.S.; Writing Original Draft Preparation: P.S., L.S., and M.B.; Writing Review and Editing: L.S., P.S., and M.B.; Visualization: P.S. All authors have read and agreed to the published version of the manuscript.

6.2. Data Availability Statement

The data presented in this study are available on request from the corresponding author.

6.3. Funding

The authors received no financial support for the research, authorship, and/or publication of this article.

6.4. Institutional Review Board Statement

Not applicable.

6.5. Informed Consent Statement

Not applicable.

6.6. Declaration of Competing Interest

The authors declare that they have no known competing financial interests or personal relationships that could have appeared to influence the work reported in this paper.

References

[1] N. Subhani, Z. May, M. K. Alam, I. Khan, M. A. Hossain, and S. Mamun, "An Improved Non-Isolated Quadratic DC-DC Boost Converter With Ultra High Gain Ability," *IEEE Access*, vol. 11, no. 1, pp. 11350–11363, 2023, doi: 10.1109/ACCESS.2023.3241863.

[2] R. V. Damodaran, H. Shareef, K. S. P. Kiranmai, and R. Errouissi, "Two-Switch Boost Converter With Improved Voltage Gain and Degree of Freedom of Control," *IEEE Access*, vol. 11, no. 1, pp. 23827–23838, 2023, doi: 10.1109/ACCESS.2023.3249107.

[3] S. Pirpoor, S. Rahimpour, M. Andi, N. Kanagaraj, S. Pirouzi, and A. H. Mohammed, "A Novel and High-Gain Switched-Capacitor and Switched-Inductor-based DC/DC Boost Converter with Low Input Current Ripple and Mitigated Voltage Stresses," *IEEE Access*, vol. 2022, no. 1, pp. 1–1, 2022, doi: 10.1109/ACCESS.2022.3161576.

[4] M. A. Al-Saffar and E. H. Ismail, "A High Voltage Ratio and Low Stress DC–DC Converter with Reduced Input Current Ripple for Fuel Cell Source," *Renewable Energy*, vol. 82, no. 1, pp. 35–43, 2015, doi: 10.1016/j.renene.2014.08.020.

[5] M. Forouzesh, Y. P. Siwakoti, S. A. Gorji, F. Blaabjerg, and B. Lehman, "Step-Up DC–DC Converters: A Comprehensive Review of Voltage-Boosting Techniques, Topologies, and Applications," *IEEE Transactions on Power Electronics*, vol. 32, no. 12, pp. 9143–9178, 2017, doi: 10.1109/TPEL.2017.2652318.

[6] F. Blaabjerg and D. M. Ionel, "Renewable Energy Devices and Systems – State-of-the-Art Technology, Research and Development, Challenges and Future Trends," *Electric Power Components and Systems*, vol. 43, no. 12, pp. 1319–1328, 2015, doi: 10.1080/15325008.2015.1062819.

[7] A. Allehyani, "Analysis of A Transformerless Single Switch High Gain DC–DC Converter for Renewable Energy Systems," Arabian Journal for Science and Engineering, vol. 46, no. 10, pp. 9691–9702, 2021, doi: 10.1007/s13369-021-05472-3.

[8] M. Rezvanyvardom, "Interleaved Step-Up Soft-Switching DC–DC Boost Converter without Auxiliary Switches," *Energy Reports*, vol. 8, no. 1, pp. 6499–6511, 2022, doi: 10.1016/j.egyr.2022.04.069.

[9] L. Yang, W. Yu, and J. Zhang, "High Voltage Gain Ratio Isolated Resonant Switched-Capacitor Converter for Sustainable Energy," *IEEE Access*, vol. 7, no. 1, pp. 23055–23067, 2019, doi: 10.1109/ACCESS.2019.2893981.

[10] S.-W. Seo, J.-H. Ryu, H. H. Choi, and J.-B. Lee, "Input-Parallel Output-Series High Step-Up DC/DC Converter With Coupled Inductor and Switched Capacitor," *IEEE Access*, vol. 11, no. 1, pp. 89164–89179, 2023, doi: 10.1109/ACCESS.2023.3302350.

[11] H. Tarzamni, H. S. Gohari, M. Sabahi, and J. Kyyrä, "Non-Isolated High Step-Up DC-DC Converters: Comparative Review and Metrics Applicability," *IEEE Transactions on Power Electronics*, vol. 2023, no. 1, pp. 1-11, 2023, doi: 10.1109/TPEL.2023.3264172.

[12] S. Khan, A. Mahmood, M. Tariq, M. Zaid, I. Khan, and S. Rahman, "Improved Dual Switch Non-Isolated High Gain Boost Converter for DC Microgrid Application," *2021 IEEE Texas Power and Energy Conference (TPEC)*, vol. 2021, no. 1, pp. 1–6, 2021, doi: 10.1109/TPEC51183.2021.9384956.

[13] J. Ahmad, "A New High-Gain DC-DC Converter with Continuous Input Current for DC Microgrid Applications," *Energies*, vol. 14, no. 9, pp. 2629-2640, 2021, doi: 10.3390/en14092629.

[14] J. Ahmad, "A New High Voltage Gain DC to DC Converter with Low Voltage Stress for Energy Storage System Application," *Electronics*, vol. 9, no. 12, pp. 2067-2078, 2020, doi: 10.3390/electronics9122067.

[15] R. R. Kumar, "Switched-LC Based High Gain Converter With Lower Component Count," *IEEE Transactions on Industry Applications*, vol. 56, no. 3, pp. 2816–2827, 2020, doi: 10.1109/TIA.2020.2980215.

[16] M. M. Haji-Esmaeili, E. Babaei, and M. Sabahi, "High Step-Up Quasi-Z Source DC–DC Converter," *IEEE Transactions on Power Electronics,* vol. 33, no. 12, pp. 10563–10571, 2018, doi: 10.1109/TPEL.2018.2810884.

[17] P. Kumar and M. Veerachary, "Z-Network Plus Switched-Capacitor Boost DC–DC Converter," *IEEE Journal of Emerging and Selected Topics in Power Electronics*, vol. 9, no. 1, pp. 791–803, 2019, doi: 10.1109/JESTPE.2019.2959078.

[18] A. Chub, D. Vinnikov, E. Liivik, and T. Jalakas, "Multiphase Quasi-Z-Source DC–DC Converters for Residential Distributed Generation Systems," *IEEE Transactions on Industrial Electronics*, vol. 65, no. 10, pp. 8361–8371, 2018, doi: 10.1109/TIE.2018.2801860.

[19] M. Meraj, M. S. Bhaskar, A. Iqbal, N. Al-Emadi, and S. Rahman, "Interleaved Multilevel Boost Converter With Minimal Voltage Multiplier Components for High-Voltage Step-Up Applications," *IEEE Transactions on Power Electronics*, vol. 35, no. 12, pp. 12816–12833, 2020, doi: 10.1109/TPEL.2020.2992602.

[20] S. Khan, M. Zaid, A. Mahmood, J. Ahmad, and A. Alam, "A Single Switch High Gain DC-DC Converter with Reduced Voltage Stress," *2021 IEEE 8th Uttar Pradesh Section International Conference on Electrical, Electronics and Computer Engineering (UPCON),* vol. 8, no. 1, pp. 1-7, 2020, doi: 10.1109/UPCON50219.2020.9376578.

[21] F. M. Shahir, E. Babaei, and M. Farsadi, "Analysis and Design of Voltage-Lift Technique-Based Non-Isolated Boost DC–DC Converter," *IET Power Electronics*, vol. 11, no. 6, pp. 1083–1091, 2018, doi: 10.1049/iet-pel.2017.0259.

[22] A. M. S. S. Andrade, T. Faistel, R. A. Guisso, and A. Toebe, "Hybrid High Voltage Gain Transformerless DC-DC Converter," *IEEE Transactions on Industrial Electronics*, vol. 2021, no. 1, pp. 1-7, 2021, doi: 10.1109/TIE.2021.3066939.

[23] M. Zaid, "A Transformerless High Gain DC–DC Boost Converter with Reduced Voltage Stress," *International Transactions on Electrical Energy Systems*, vol. 31, no. 5, pp. 1-7, 2021, doi: 10.1002/2050-7038.12877.

[24] W. Y. Leong, "Digital Technology for ASEAN Energy," *2023 IEEE International Conference on Communication and Power Engineering (ICCPE)*, vol. 2023, no. 1, pp. 1-7, 2023, doi: 10.1109/ICCPCT58313.2023.10244806.